AD-A095 173 WEIDLINGER ASSOCIATES NEW YORK F/G 11/6
NUMERICAL STUDIES OF TENSION MODELS: INSTANTANEOUS FRACTURE, PL--ETC(U)
JUL 78 L WHITMAN, J P WRIGHT DNA001-77-C-0035

UNCLASSIFIED DNA-5330Z NL

1 OF 1
AD
A095 173

END
DATE
FILMED
3-81
DTIC

AD A095173

DNA 5330Z

NUMERICAL STUDIES OF TENSION MODELS: INSTANTANEOUS FRACTURE, PLASTIC FAILURE, RATE-DEPENDENT DAMAGE ACCUMULATION

Weidlinger Associates, Consulting Engineers
110 East 59th Street
New York, New York 10022

1 July 1978

Interim Report for Period 20 October 1976—1 July 1978

CONTRACT No. DNA 001-77-C-0035

APPROVED FOR PUBLIC RELEASE;
DISTRIBUTION UNLIMITED.

THIS WORK SPONSORED BY THE DEFENSE NUCLEAR AGENCY
UNDER RDT&E RMSS CODE B344077464 Y99QAXSB25504 H2590D.

Prepared for
Director
DEFENSE NUCLEAR AGENCY
Washington, D. C. 20305

Destroy this report when it is no longer needed. Do not return to sender.

PLEASE NOTIFY THE DEFENSE NUCLEAR AGENCY, ATTN: STTI, WASHINGTON, D.C. 20305, IF YOUR ADDRESS IS INCORRECT, IF YOU WISH TO BE DELETED FROM THE DISTRIBUTION LIST, OR IF THE ADDRESSEE IS NO LONGER EMPLOYED BY YOUR ORGANIZATION.

REPORT DOCUMENTATION PAGE

READ INSTRUCTIONS BEFORE COMPLETING FORM

1. REPORT NUMBER: DNA 5330Z
2. GOVT ACCESSION NO.: AD-A095 173
3. RECIPIENT'S CATALOG NUMBER:
4. TITLE (and Subtitle): NUMERICAL STUDIES OF TENSION MODELS: INSTANTANEOUS FRACTURE, PLASTIC FAILURE, RATE-DEPENDENT DAMAGE ACCUMULATION.
5. TYPE OF REPORT & PERIOD COVERED: Interim Report ~~for Period~~ 20 Oct 76—1 Jul 78
6. PERFORMING ORG. REPORT NUMBER:
7. AUTHOR(s): Lorraine Whitman, Joseph P. Wright
8. CONTRACT OR GRANT NUMBER(s): DNA 001-77-C-0035
9. PERFORMING ORGANIZATION NAME AND ADDRESS: Weidlinger Associates, Consulting Enginee, 110 East 59th Street, New York, New York 10022
10. PROGRAM ELEMENT, PROJECT, TASK AREA & WORK UNIT NUMBERS: Subtask Y99QAXSB255-04
11. CONTROLLING OFFICE NAME AND ADDRESS: Director, Defense Nuclear Agency, Washington, D.C. 20305
12. REPORT DATE: 1 July 1978
13. NUMBER OF PAGES: 40
14. MONITORING AGENCY NAME & ADDRESS (if different from Controlling Office):
15. SECURITY CLASS. (of this report): UNCLASSIFIED
15a. DECLASSIFICATION/DOWNGRADING SCHEDULE:
16. DISTRIBUTION STATEMENT (of this Report): Approved for public release; distribution unlimited.
17. DISTRIBUTION STATEMENT (of the abstract entered in Block 20, if different from Report):
18. SUPPLEMENTARY NOTES: This work sponsored by the Defense Nuclear Agency under RDT&E RMSS Code B344077464 Y99QAXSB25504 H2590D.
19. KEY WORDS (Continue on reverse side if necessary and identify by block number):

Uniqueness	Tension Models
Stability	Geological Material
Rate Effects	Ground Shock

20. ABSTRACT (Continue on reverse side if necessary and identify by block number)

As part of a continuing study of tension models for ground shock calculations, two rate-independent models (instantaneous fracture and plastic failure) are re-examined. Neither model combines the two desired traits of stability-uniqueness and physical realism.

Instead, a modified rate-dependent model is proposed for brittle tensile failure in ground shock calculations. It is based on the ductile damage accumulation equations advanced at SRI and Sandia, but in simplified,

20. ABSTRACT (Continued)

fully incremental form.

Preliminary uniaxial strain calculations show the model to give physically realistic results, close to the predictions of the more complicated rate-dependent model BFRACT. Further testing of the model for more realistic two dimensional problems and an analysis of cost versus benefit is in progress.

TABLE OF CONTENTS

A

LIST OF ILLUSTRATIONS

I INTRODUCTION

In an earlier report, Ref. [1], the present authors considered the possibility of improving the tensile modeling of geological materials by adopting the SRI rate-dependent brittle fracture model BFRACT. It was concluded that the model was too costly for the large-scale ground shock problems of interest, due to the large number of memory parameters required.

It was recommended then that versions of the instantaneous tensile fracture model commonly in use be re-evaluated. These versions are mathematically discontinuous (since some stress quantity is instantaneously reset to zero when the tensile strength of the material is exceeded) and hence are prone to stability-uniqueness problems. Such procedures have been employed for many years, presumably without any numerical instabilities being traced to their use. However, it has been noted that arbitrarily small differences in input data do lead, on occasion, to significantly altered wave forms. It was further recommended that a plasticity model be tested to see if it is an adequate alternative representation for tensile failure in ground shock calculations.

To study these recommendations some simple one-dimensional wave propagation calculations were made. The anticipated shortcomings, for both instantaneous fracture and plasticity models, are documented. No method has evolved for amending the rate-independent models to overcome these shortcomings.

Instead, for both physical and theoretical reasons, a rate-dependent model for brittle tensile fracture in ground shock calculations is proposed. The model adds only one additional state variable, the relative void volume or damage, to a viscoplastic-like description of material in tension. It is based on the ductile damage accumulation equations advanced at SRI and Sandia, but in simplified and fully incremental form.

Preliminary uniaxial strain calculations show the model to give physically reasonable results and, in fact, to predict stress-strain paths quite close to those of the more complicated and detailed model BFRACT. Further testing of the model, for more realistic two-dimensional problems, and a study of cost versus benefit in ground shock calculations is in progress.

II RATE-INDEPENDENT MODELS

A. Exact Solutions

A compressive step pulse of width ℓ and amplitude s (negative in compression) is assumed to propagate toward the free surface of a semi-infinite bar of linear elastic material (see Fig. 1). The particle velocity v_o is then $(s/\rho c)$ toward the left with ρ the undisturbed density and c the wave speed. The exact solution of the problem, for times greater than the time of wave reflection, is critically dependent upon the strength of the pulse relative to the tensile strength of the material σ_o .

For an incoming pulse such that $-s < \sigma_o$ a tensile wave of amplitude $-s$ reflects back down the bar.

For $-s > \sigma_o$ the ideal solution is a function of the tensile failure option. Assuming instantaneous fracture with all stress quantities reset to zero, a piece of length $\ell/2$ spalls off with uniform velocity equal to twice the incoming particle velocity; the remainder of the bar is at rest. Assuming plastic tensile failure (as implemented in the cap model routine, Ref. [2]), the exact solution is a broadened, reduced tensile pulse, of the form indicated in Fig. 1,*) returned by the free end of the bar. It is clear that the plastic solution is not a physically realistic model for tensile fracture. (The exact solutions for all cases under consideration are illustrated in Fig. 1.)

B. Numerical Tests

Using the finite difference wave propagation code WONDY, Ref. [3], the numerical solutions obtained for the step pulse problem differ from the exact solutions discussed above in ways generally characteristic of numerical solutions. The initial square wave becomes rounded. Small amplitude numerical oscillations appear, causing local "overshoots" and "undershoots". Where a

*) Private communication, I.S. Sandler, Weidlinger Associates.

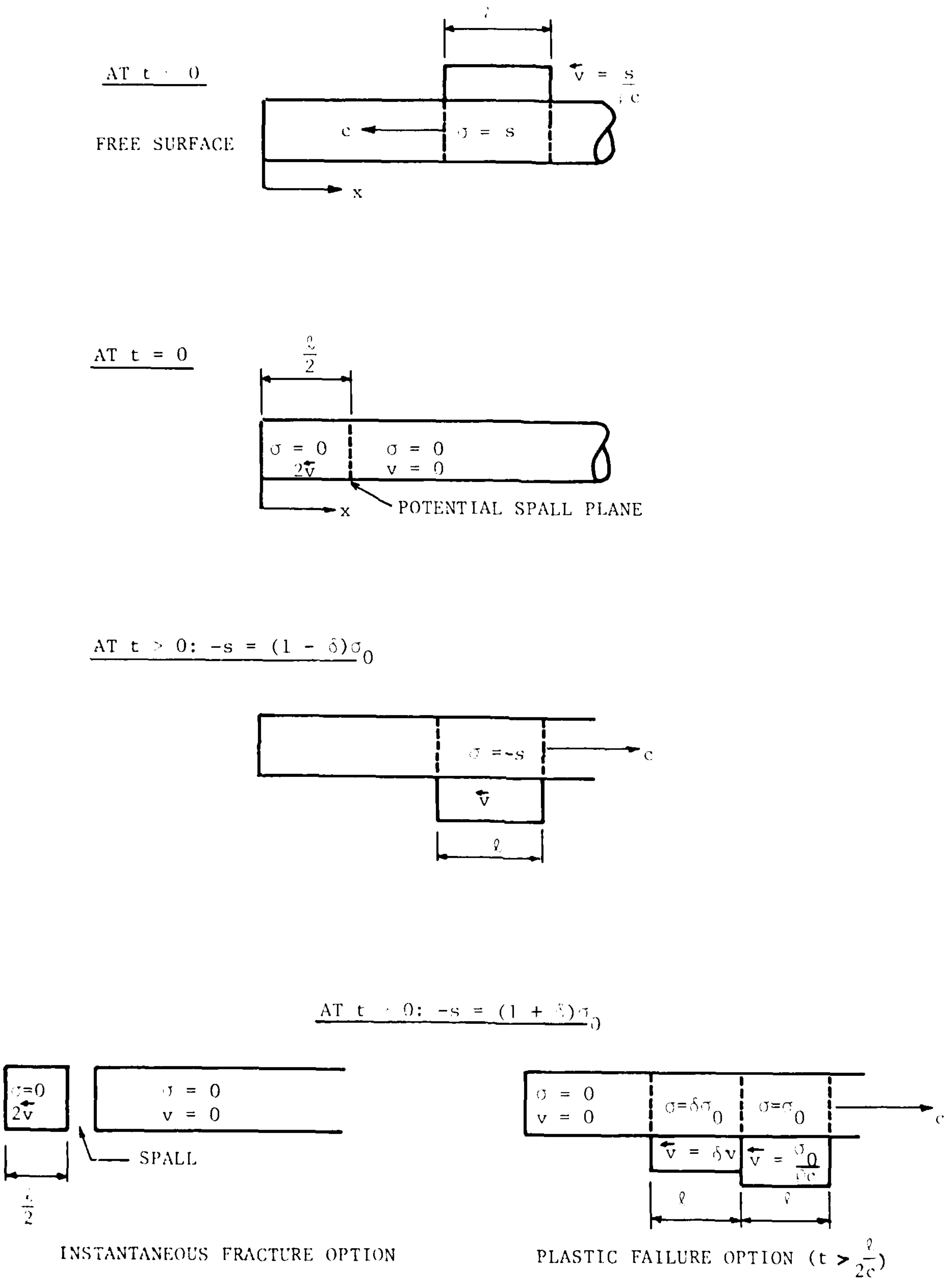

Fig. 1 Step Pulse Propatating Along a Semi-Infinite Bar of Linear Elastic Material.

spall segment forms, its velocity profile is not ideally flat-topped. For models with stability-uniqueness problems, these numerical deviations can have significant consequences.

Instantaneous fracture can be implemented in pure continuum fashion or by introducing an additional node and permitting separation as is done in WONDY, when the tensile strength of a material is exceeded, for example. Similar problems arise in either case. The former option has been selected for the present numerical test along with the following non-dimensionalized sample data: $\rho = 1$, $c = 1$, $\sigma_o = 0.0296$, $\ell = 0.4$. In non-dimensionalized units then, the initial particle velocity is equal to the incoming stress pulse, $v_o = s$. (Additional details of the code implementation are given in Appendix A.)

In Fig. 2 an initial square pulse, with $v_o = 0.90\ \sigma_o$, is shown.*) At a later time, $t = 0.85$, the particle velocity is seen to have approximately doubled at the free end of the bar. At twice the previous time, $t = 1.7$, the wave has reflected back in tension. Ignoring the numerical inaccuracies discussed previously, the ideal solution for a pulse of amplitude less than the tensile strength of the material has been obtained.

Increasing the initial pulse velocity (synonomous with increasing the stress) a small amount to $0.92\ \sigma_o$ causes the ideal solution to be lost. For such initial data the third time frame ($t = 1.7$) in Fig. 3 shows the physically unrealistic formation of a spall segment. Instantaneous tensile fracture has been triggered as the numerical overshoots, expected to develop in the finite difference solution, produce a local stress level in excess of σ_o .

---

*) The minus sign to indicate travel toward the left is henceforth suppressed.

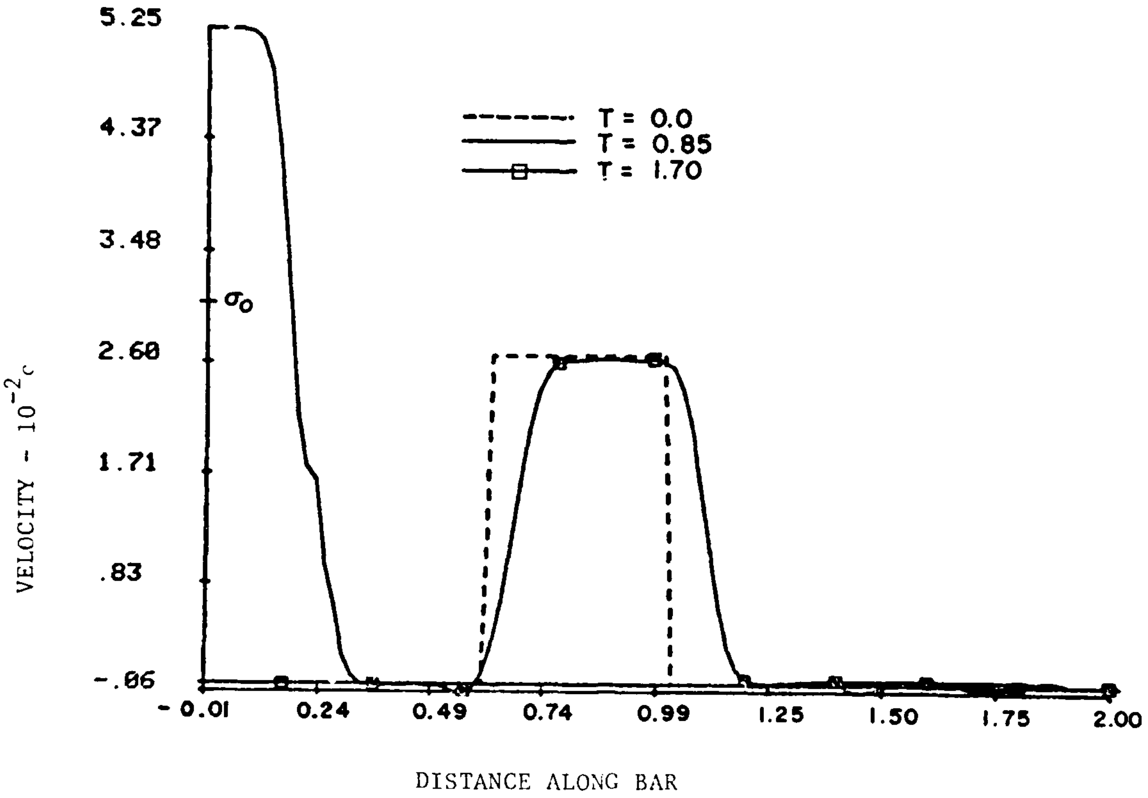

Fig. 2 Instantaneous Tensile Fracture. $v_o = 0.90\ \sigma_o$

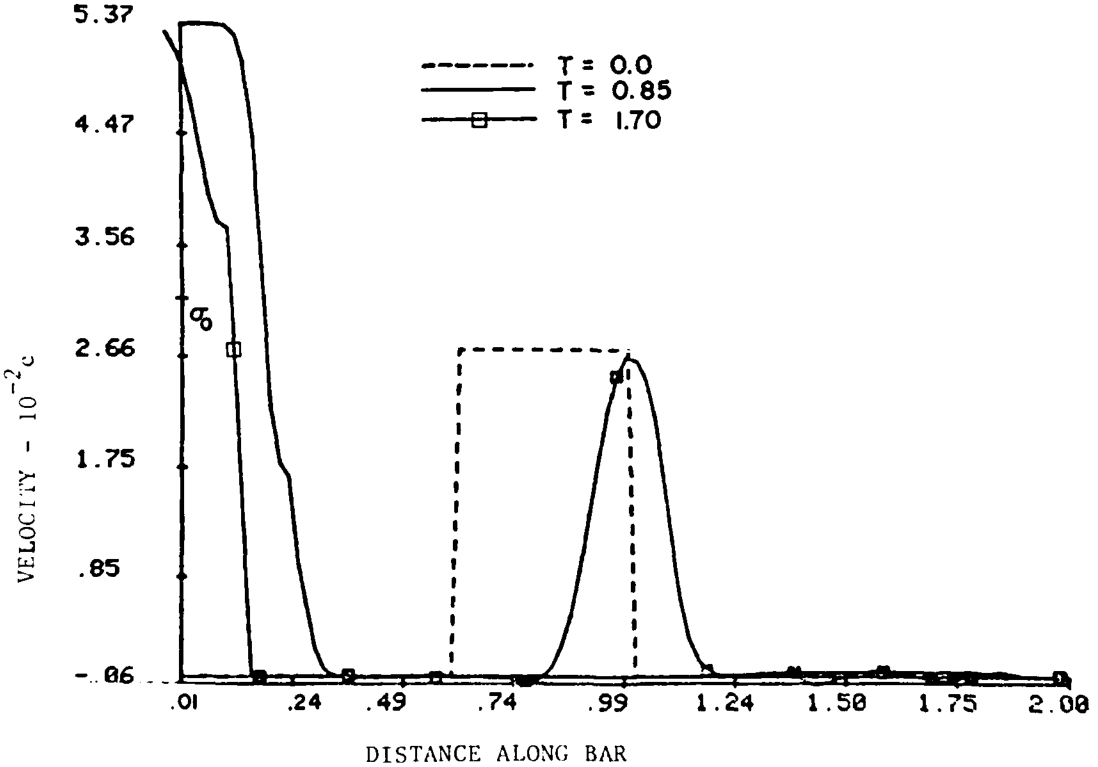

Fig. 3 Instantaneous Tensile Fracture. $v_o = 0.92\ \sigma_o$

A small change in input data is seen to produce a large, non-physical, change in the results.

Purely computational parameters, unrelated to the input data of the physical problem, can be shown to unduly influence results as well. These computational parameters arise in the consideration of artificial viscosity and time step selection.

Two types of artificial viscosity are added in WONDY under locally compressive situations, $\dot{\rho} > 0$. The quadratic form of artificial viscosity

$$q_1 = B_1^2 \left(\frac{\dot{\rho}}{\rho}\right)^2 \rho \Delta x^2$$

is most effective in controlling gradients at shocks while introducing mimimal disturbances elsewhere. The linear form,

$$q_2 = B_2 \, c\dot{\rho} \, \Delta x$$

is used to control the high frequency oscillations, though with great care as this form is prone to distort a general solution away from shock areas as well as close in. B_1 and B_2 are the quadratic and linear artificial viscosity coefficients and Δx is a cell width. To insure general numerical stability the time step used to advance the computation is controlled by a Courant-Friedrichs-Lewy type of condition, Ref. [3],

$$\Delta t = k \begin{cases} \dfrac{\Delta x}{c} & , \quad \text{for } \dfrac{\dot{\rho}}{\rho} \leq 0 \\[2ex] \dfrac{\Delta x}{B_2 c + B_1^2 \dfrac{\dot{\rho}}{\rho} \Delta x + \sqrt{\left(B_2 c + B_1^2 \dfrac{\dot{\rho}}{\rho} \Delta x\right)^2 + c^2}} & , \quad \text{for } \dfrac{\dot{\rho}}{\rho} > 0 \end{cases}$$

The numerical parameter k is the Courant number, lying between 0 and 1. In general k is taken close to 1 to maximize the possible time step, while k equal to 1, marginal stability, is avoided. Default values in WONDY for

B_1, B_2 and k are 2.0, 0.1 and 0.98, respectively. These values are assumed unless otherwise stated.

In Fig. 4 the incoming pulse velocity is again $v_o = 0.90\ \sigma_o$, but k has been reduced to 0.49 and spall once more appears. Smaller time steps have anomalously produced a less physically accurate result, one which appears, for this particular configuration, analogous to running with a reduced amount of artificial viscosity. (This is not a general result, but another manifestation of the instantaneous fracture model's theoretical deficiency.)

Spall can be suppressed (local overshoots reduced), by increasing the strength of the artificial viscosity while all other quantities are held constant. In Fig. 5, B_2 has been increased from 0.1 to 1.0, v_o being $0.90\ \sigma_o$ and k being 0.49. With this set of parameters a tensile wave is once again observed to propagate back from the free end of the bar as required physically, though in this case it is observably damped.

Table 1 summarizes the results obtained for the step pulse problem run with instantaneous tensile fracture for the four sets of parameters discussed above.

Table 1. Step Pulse Problem with Instantaneous Tensile Fracture.

Incoming Stress Level $-s/\sigma_o$	Courant Number k	Artificial Viscosity Coefficient Quadratic B_1	Linear B_2	Spall Fragment Formation
0.90	0.98	2.0	0.1	No
0.92	0.98	2.0	0.1	Yes
0.90	0.49	2.0	0.1	Yes
0.90	0.49	2.0	1.0	No

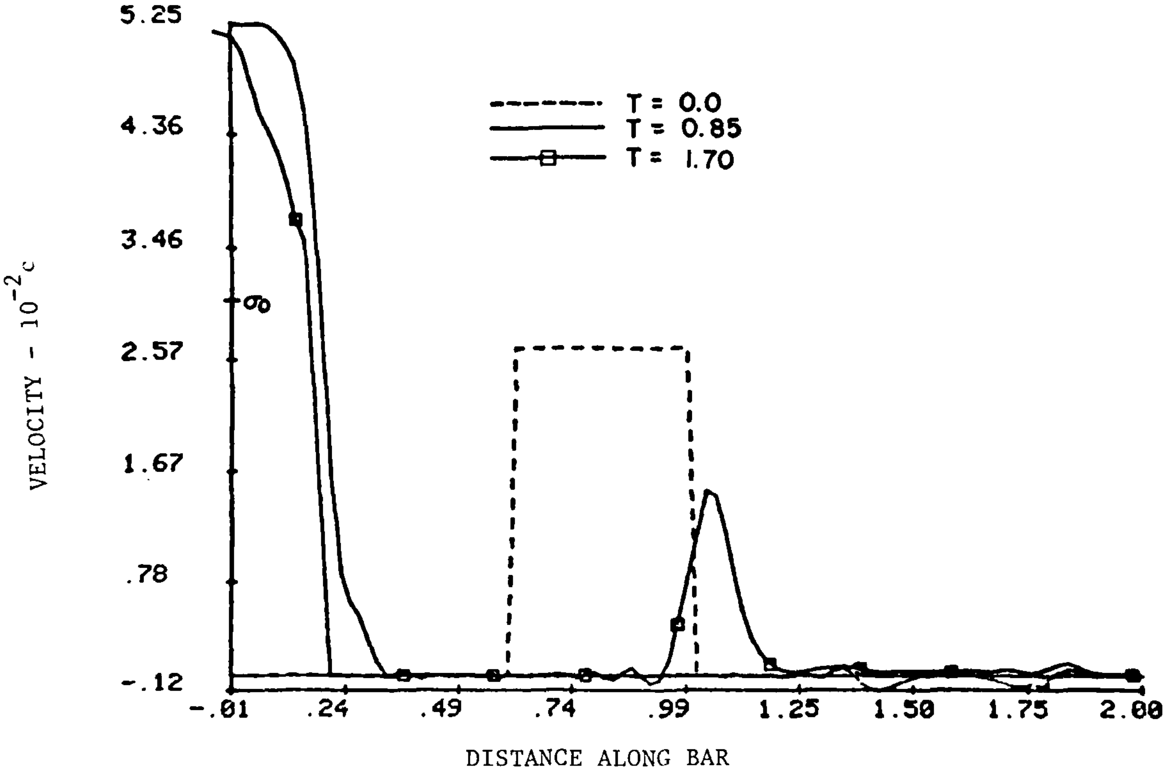

Fig. 4 Instantaneous Tensile Fracture. $v_o = 0.90\ \sigma_o$
Courant Number Halved.

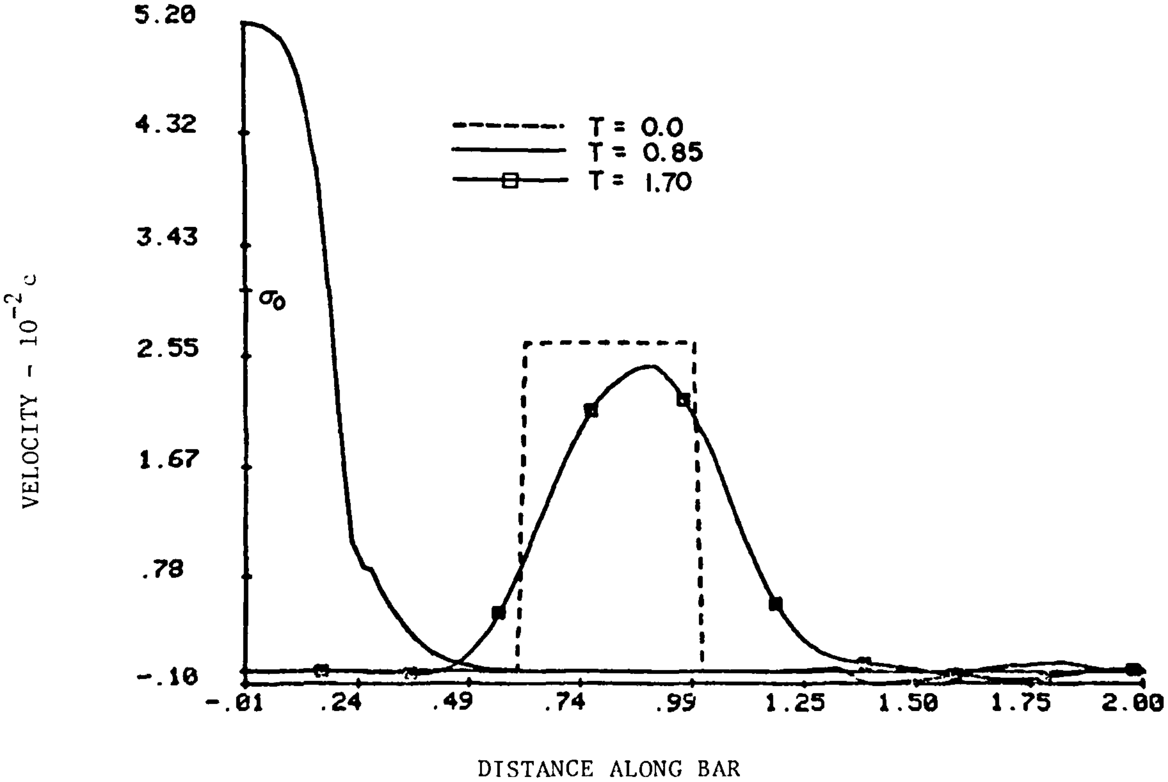

Fig. 5 Instantaneous Tensile Fracture. $v_o = 0.90\ \sigma_o$
Courant Number Halved. Linear Artificial Viscosity Increased Tenfold.

When the square wave problem is solved exactly with a plasticity model of tensile failure no spall fragment forms, whatever the initial stress level. Since the set of constitutive equations is well-behaved, it can be anticipated that the numerical results will closely match the theoretical. At an incident stress level 50% above σ_o a primary tensile wave of width ℓ and amplitude σ_o, followed by a secondary wave of width ℓ and amplitude $\sigma_o/2$, is the predicted solution*). This wave form, as shown in Fig. 6, is approximately obtained numerically. In contrast, the required physical solution, spall, is seen in Fig. 7 where instantaneous tensile fracture has been assumed and $-s$ is again 50% above σ_o.

As expected, for this highly idealized problem (and for any ground shock calculation where spall is expected to be important), neither rate-independent model of tensile failure satisfies both the requirements of stability-uniqueness and of physical realism. Rather than attempt to amend the rate-independent models, the choice has been made to develop a highly simplified rate-dependent model as a way of overcoming the discussed shortcomings.

---

*) Refer back to Fig. 1 for the general form of the plastic failure solution for $-s > \sigma_o$.

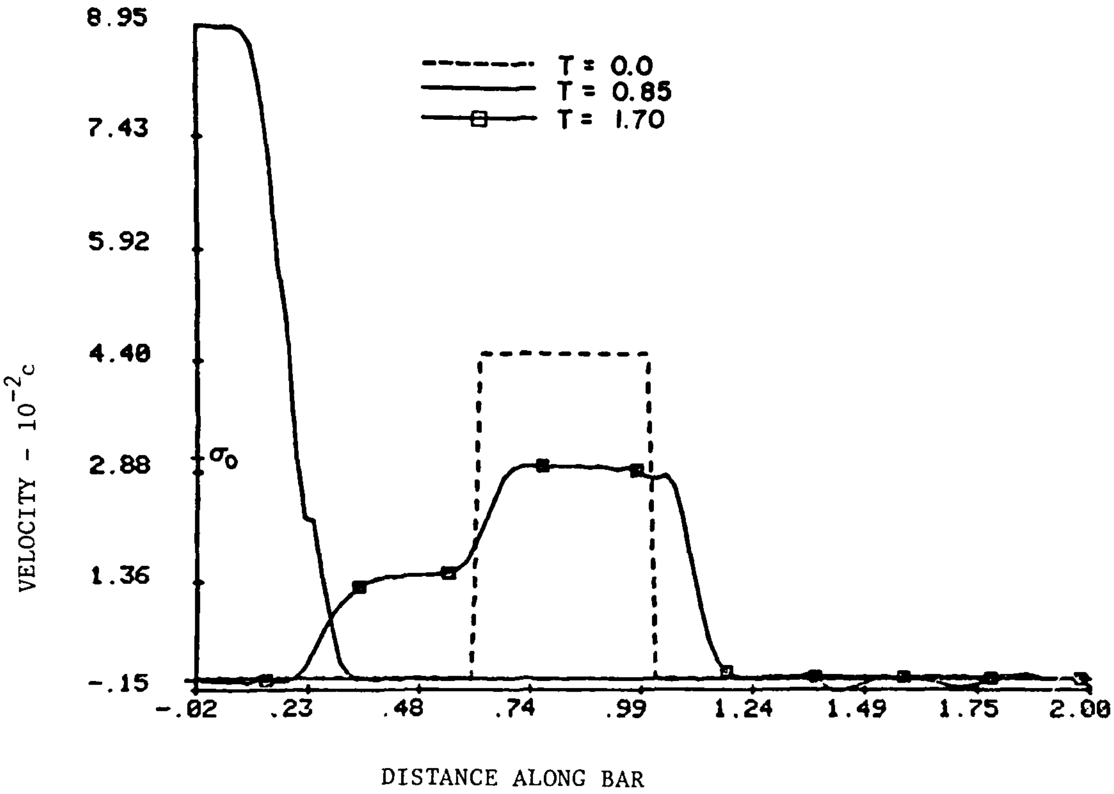

Fig. 6 Plastic Tensile Failure. $v_o = 1.5\ \sigma_o$

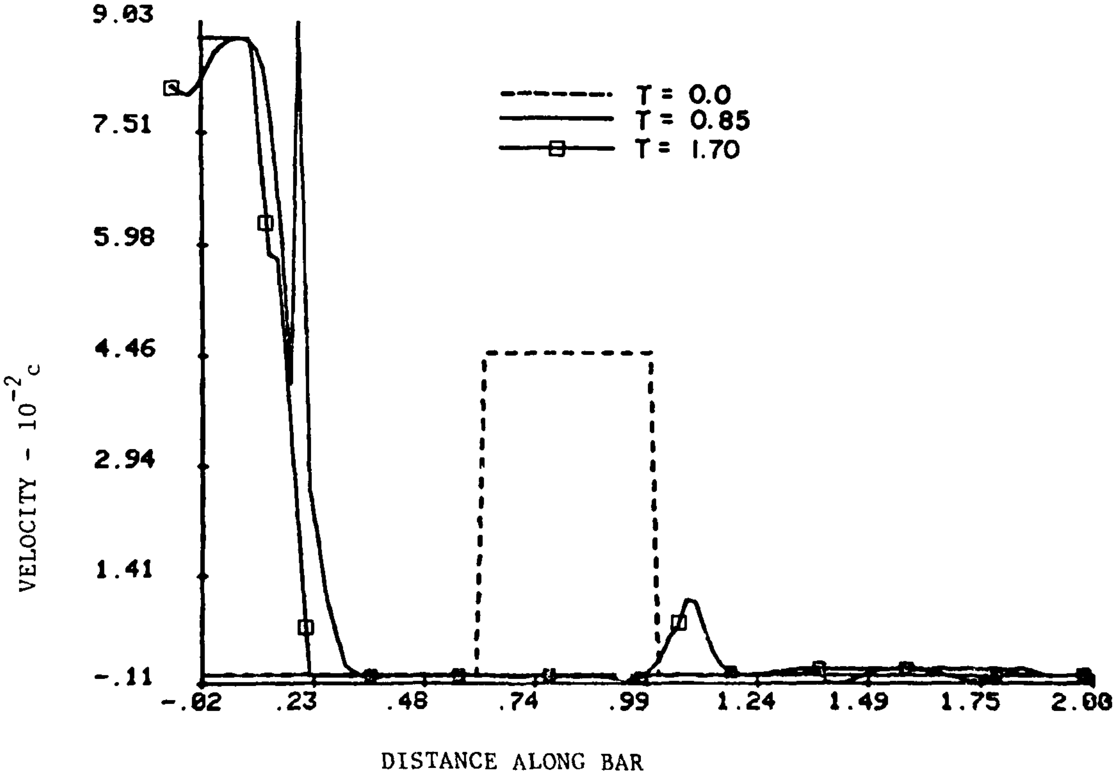

Fig. 7. Instantaneous Tensile Fracture. $v_o = 1.5\ \sigma_o$

III RATE-DEPENDENT MODELS

A. Weidlinger Visco-Damage Model

An alternative to the rate-independent or multi-parameter rate-dependent models previously discussed is suggested. As compared to SRI-BFRACT, Ref. [4], or to the brittle spallation theory of Davison and Stevens, Ref. [5], the simplifying assumption is made that a single volumetric state variable D, the tension-induced relative void volume or damage, is sufficient to characterize tensile fracture. By not recording the varying sizes and orientations of planar cracks (actually found in bittle materials) it is felt that computational costs can be sufficiently reduced to make a rate-dependent, and hence mathematically stable, model practical for ground shock calculations.

It is proposed that the incremental elastic constitutive equation, $\dot{\sigma} = M_o\dot{\varepsilon}$, be modified to include the time-dependent growth of damage as follows:

$$\dot{\sigma} + \omega(\sigma,D,\varepsilon;t)\dot{D} = M(\sigma,D,\varepsilon;t)\dot{\varepsilon}, \qquad (1)$$

where σ is the average stress and ε the volumetric strain. The damage growth rate D is taken as a function of the dependent variables and time, but not of their rates

$$\dot{D} = f(\sigma,D,\varepsilon;t)$$

To satisfy continuity it is required that M reduce to the undamaged elastic modulus M_o and that the product ωD go to zero for stresses less tensile than some threshold value σ_o and for damage equal to zero. The requirements that, in a uniaxial strain test for example, time to fracture decrease and peak tensile strength increase with increasing strain-rate impose further constraints on the functional forms of σ, $\dot{D}$ and M. (Such rate dependences have been documented for rock in Ref. [6], for example.)

Unlike the various nonlinear elastic-viscoplastic constitutive equations examined, for example in Refs. [6, 7, 8], this form has been tailored to model the (rapid) relaxation of stress to zero characteristic of tensile failure, provided that $\omega\dot{D}$ remains finite (and positive) as damage increases.

The theory of spall damage accumulation in ductile metals of Davison, Stevens and Kipp, Ref. [9], of Sandia can be adapted to fit the above formalism. The Sandia model in turn relies upon the SRI fracture models discussed in Ref. [4], for spherical void size distributions and growth laws and for laboratory data to set the material parameters.

The time rate of change of damage separates into two parts, one dependent on void nucleation, the other on void growth

$$\dot{D} = \dot{D}_n + \dot{D}_G \equiv f \tag{2}$$

From Ref. [9]

$$\dot{D}_n = c_n \mathcal{V}_o \left[\exp\left[\frac{\sigma-\sigma_n + |\sigma-\sigma_n|}{2\sigma_1}\right] - 1 \right] (1-D)^2$$

and

$$\dot{D}_G = \frac{3}{2} c_G [2\sigma + |\sigma-\sigma_G| - |\sigma+\sigma_G|]\, D(1-D) \tag{3}$$

where c_n is the initial time rate of change of void volume, $\mathcal{V}_o$ the average initial (spherical) void volume, σ_n the nucleation threshold, σ_1 the nucleation sensitivity, c_G the growth coefficient and σ_G the growth threshold. These material parameters can be related to the SRI material constants, T_1 to T_6, as indicated in Appendix B. (Stress and strain are assumed positive in tension.)

An integrated form has been assumed in Ref. [9] for the average stress in the small strain approximation,

$$\sigma = K\varepsilon \tag{4}$$

with the volumetric strain ε and the bulk modulus K both taken as damage-dependent quantities. In particular, for the case of uniaxial strain and for ρ_R a reference density,

$$\varepsilon(\rho, D) = [(2 + \rho_R/\rho)(1-D)^{1/3} - 3]$$

has been obtained*). The bulk modulus of a composite material at low damage levels, Ref. [10], is assumed with ν_o the Poisson ratio and K_o the undamaged modulus,

$$K = K_o[1 - \frac{3(1-\nu_o)}{2(1-2\nu_o)} D]$$

For ν_o equal to 1/3, the expression becomes

$$K = K_o(1 - 3D) \tag{5}$$

In this case, damage is constrained to be less than or equal to a third.

Differentiating Eq. (4) with respect to time and reverting to a damage-independent concept of strain, one may write

$$\dot{\sigma} + \dot{K}\varepsilon + K\dot{\varepsilon}$$

or

$$\dot{\sigma} + 3K_o\varepsilon\dot{D} = K\dot{\varepsilon} \;, \quad D < 1/3 \tag{6}$$

The following identifications can then be made for the unknown functions in Eq. (1)

$$\omega(\sigma,D,\varepsilon;t) = 3K_o\varepsilon$$

$$M(\sigma,D,\varepsilon;t) = K$$

completing the specification of the proposed rate-dependent volumetric stress-strain relation for material in tension.

Examining Eqs. (1)-(3), it is clear that damage initiation is controlled by the nucleation threshold σ_n for the usual case $D(t=0) = 0$. On the other hand, stress relaxation can continue, for increasing tensile strain and large damage values ($D \to 1/3$), until the lower of the two threshold stresses, σ_n of σ_G is reached. Depending upon how stringently the requirements of relaxation to zero stress for brittle fracture is to be met, σ_G may be taken anywhere from an order of magnitude or two less than σ_n to zero, to give the appropriate

---

*) Actually, the Sandia form is more complex. Thermal effects and plastic flow have also been accounted for in the strain components. These are being disregarded as not relevant to the present investigation.

asymptotic stress behavior without affecting the onset of damage accumulation.*)

B. SRI Ductile Fracture Model

While the routine BFRACT has been used to model tensile fracture in a ground shock test calculation, Ref. [11], the closest to the proposed rate-dependent model for such calculations may well be the simpler, less time consuming routine DFRACT, Ref. [4], constructed for ductile materials. This model requires the calculation of solid specific volume and pressure in addition to gross specific volume and pressure. It accounts for the progressive growth of damage, in the form of spherical voids, and for the relaxation of stress under the influence of continuing tensile strain. Details of the model are given in Appendix B.

The main advantage of the proposed Weidlinger visco-damage model is that it is expressed in incremental form and, hence, mathematically better understood. *Also, it requires the storage of* fewer memory parameters per computational cell, corresponding to the introduction of one, rather than two, additional state variables.

C. Numerical Tests

If a constant uniaxial strain-rate is assumed, $\dot{\varepsilon}(t) = \dot{\varepsilon}_o$, the set of Weidlinger visco-damage constitutive equations becomes

$$\frac{dD}{d\varepsilon} = \frac{f}{\dot{\varepsilon}_o}$$

$$\frac{d\sigma}{d\varepsilon} = K_o[1 - 3(D + \frac{\varepsilon f}{\dot{\varepsilon}_o})]$$

with the function f given by Eqs. (2) and (3) and D in the range 0 to 1/3.

*) The parameter c_G may have to be adjusted as well to achieve full relaxation within a reasonable time interval.

Adding damage accumulation concepts to a conventional description of the deviator stresses limited by a Mises yield condition, as in Ref. [4], gives

$$ds_{ij} = 2\mu(d\varepsilon_{ij} - \frac{1}{3}\,\delta_{ij}\,\frac{dV}{V})$$

$$2J_2' = \sum s_{ij}^2 \leq \frac{2}{3}\,Y^2$$

with

$$\mu = \mu_o(1 - 1.88D)$$

and

$$Y = Y_o(1 - 4D)$$

Numerically integrating*) the resulting set of equations for a given material yields a set of strain-rate dependent stress-strain curves.

The results of such numerical integration for the brittle metal Armco iron, using SRI adapted data as listed in Appendix C, are shown in Fig. 8. These axial stress-strain curves conform well to the requirements set forth in Section A for brittle tensile fracture. Stress appears to relax fully for large enough tensile strain**). With a failure strain ε_f inferred from Fig. 8 for each constant strain rate curve, time to fracture, $T_f = \varepsilon_f/\dot{\varepsilon}_o$, is shown in Table 2 to decrease with increasing strain-rate, while peak tensile stress σ_{max} is seen to increase correspondingly.

*) Using a fourth order Runge-Kutta scheme with the Gill modification, for example.

**) In fact stress relaxes to σ_G, a low value of stress relative to σ_{max}. Alternatively, to get true relaxation to zero, the parameter σ_G can be chosen to be zero.

Table 2. Uniaxial Extension Test, Armco Iron, Weidlinger Visco-Damage Model.

Strain Rate $\dot{\epsilon}_o$ (1/sec)	Time to Fracture T_f (μsec)	Maximum Stress σ_{max} (10^9 dyn/cm^2=0.1 GPa)
10^4	1.7	24.
10^5	0.5	54.
10^6	<0.2	71.

Though limited in this simple numerical test to uniaxial strain, the results are encouraging.

The stress-strain curves produced by BFRACT driven at various constant uniaxial strain-rates with Armco data are shown superimposed on the visco-damage curves in Fig. 9. Corresponding data has been used for both models except that a correction has been made to η_o to compensate for the *change from planar to spherical voids. (See Appendix B.)* The earlier curves, calculated with the visco-damage model, are in excellent agreement with the BFRACT curves. This is not unexpected since in a one-dimensional strain test the added complexity of crack directionality goes largely unused.

As a second trial the Weidlinger visco-damage model and BFRACT have been driven at various strain-rates to simulate the uniaxial extension test with data representing the ductile metal aluminum. Material damage parameters have been obtained from Ref. [4] and are listed in Appendix B. The two sets of curves, shown superimposed in Fig. 10, are in qualitative agreement. This is despite the fact that the SRI routine DFRACT would

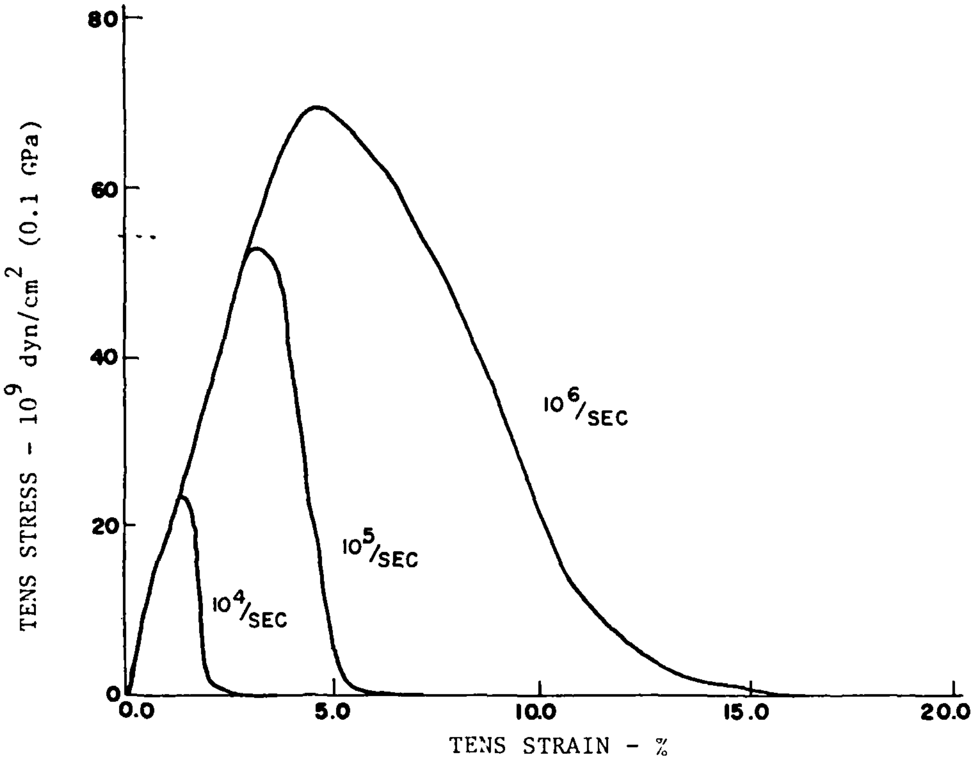

Fig. 8 Uniaxial Strain Behavior. Armco Iron. Visco-Damage Model.

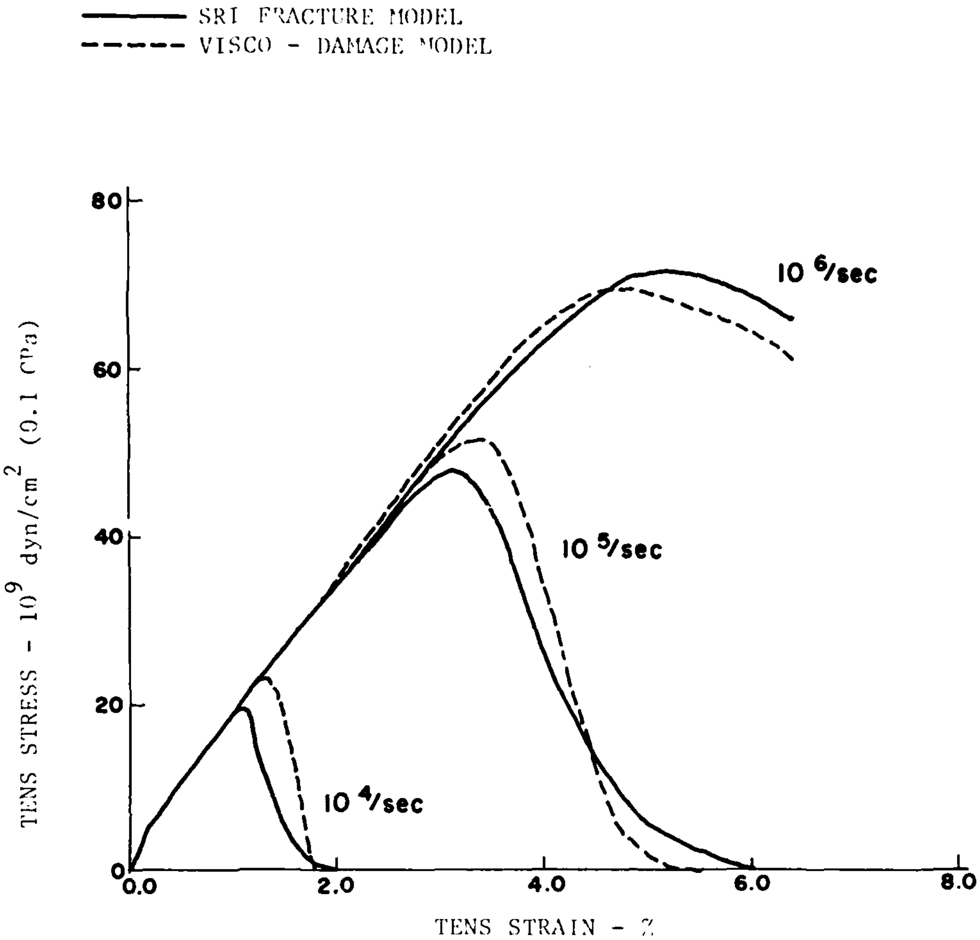

Fig. 9 Uniaxial Strain Behavior. Armco Iron.

have been the comparison model of choice for aluminum, not BFRACT[*].
Neither set of curves shows the sharp drop to zero stress characteristic of brittle tensile fracture, due to the choice of a relatively high value for σ_G, (comparable to that of σ_n). Recall from Section A that the lower of the two threshold values controls the relaxation of stress for large tensile strain and damage.

---

*) The distinction between planar cracks and spherical voids has been ignored in this trial. However, for aluminum, the models are not highly sensitive to changes in the value of the fracture parameter $\mathcal{V}_o$. In Fig. 11 $\mathcal{V}_o$ has been reduced to one-sixth of its former value, all other quantitites remaining the same. Peak tensile stress rises by less than 6%.

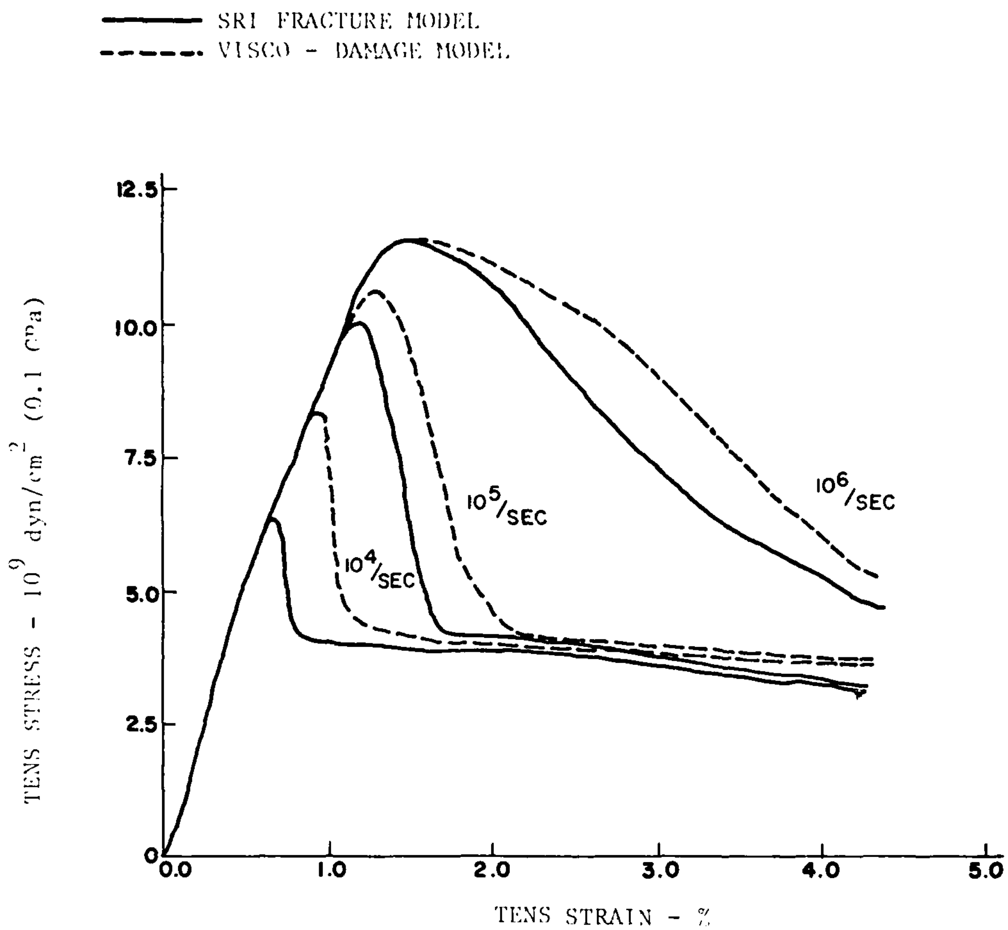

Fig. 10 Uniaxial Strain Behavior. Aluminum.

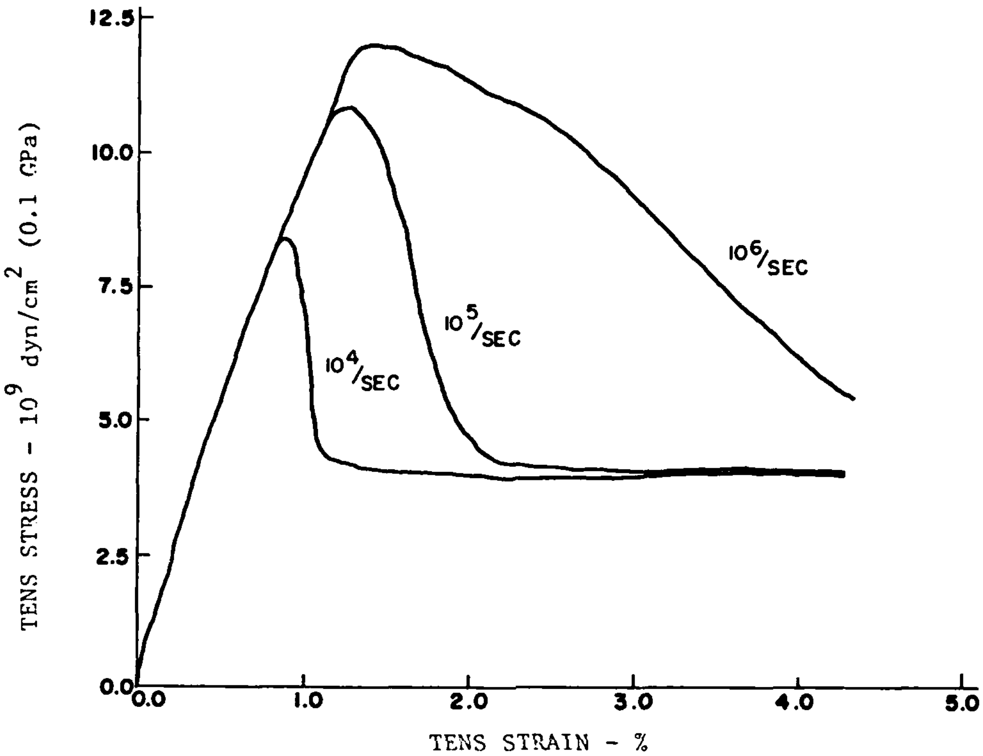

Fig. 11 Uniaxial Strain Behavior. Aluminum.
Void Volume v_o Reduced. Visco-Damage Model.

IV CONCLUSION

A. Summary

As recommended in Ref. [1], the rate-independent models - instantaneous tensile fracture and plastic failure - have been re-examined by way of a simple pulse propagation problem. Neither has been found to satisfy both the requirements of stability-uniqueness and of physical realism. A highly simplifed rate-dependent tensile fracture model, utilizing equations and material constants from SRI-DFRACT and the Sandia ductile damage accumulation model, has been proposed for use in ground shock calculations. It is formulated in fully incremental form and requires only one additional (volumetric) state variable. Preliminary uniaxial strain tests have proven encouraging.

B. Recommendations

There is a need to implement and test the Weidlinger visco-damage model in more realistic two-dimensional problems. While the model is expressed in terms of average stress and volumetric strain and is thus generalizable to multi-dimensions, it is important to test the hypothesis that a single volumetric variable is sufficient to significantly improve the modeling of brittle tensile failure. That it improves the modeling, as compared to the rate-independent models, is clear since it is mathematically well-behaved and yet physically more realistic than plastic tensile failure (particularly for rocks). Whether the additional computer cost is justified by the improvement remains to be further documented.

For problems in which crack directionality is judged to be especially important it may be possible to generalize the model with the introduction of an additional state variable. It is recommended that such an option be developed, to be used when the added computational costs seem justified by the particular site geometry.

REFERENCES

[1] Wright, J.P. and Whitman, L., "Tensile Behavior of Geological Material in Ground Shock Calculations, II", DNA 4450T, Weidlinger Associates, New York, New York, 1977.

[2] Sandler, I. and Rubin, D., "A Modular Subroutine for the Cap Model", DNA 3875F, Weidlinger Associates, New York, New York 1975.

[3] Lawrence, R.J. and Mason, D.S., "WONDY IV - A Computer Program for One-Dimensional Wave Propagation with Rezoning", SC-RR-710284, Sandia Laboratories, Albuquerque, New Mexico, 1971.

[4] Seaman, L. and Shockey, D.A., "Models for Ductile and Brittle Fracture for Two Dimensional Wave Propagation Calculations", Final Report, Contract No. DAAG46-72-C-0182, Army Materials and Mechanics Research Center, Watertown, Massachusetts, 1975.

[5] Davison, L. and Stevens, A.L., "Thermomechanical Consitution of Spalling Elastic Bodies", J. Appl. Phys., 44, 668, 1973.

[6] Grady, D.E. and Hollenbach, R.E., "Rate Controlling Processes in the Brittle Failure of Rock", SAND76-0659, Sandia Laboratories, Albuquerque, New Mexico, 1977.

[7] DiMaggio, F.L. and Sandler, I., "The Effect of Strain Rate on the Constitutive Equations of Rocks", DNA001-72-C-0003, Weidlinger Associates, New York, 1971.

[8] Cernocky, E.P. and Krempl, E., "A Nonlinear Uniaxial Integral Constitutive Equation Incorporating Rate Effects, Creep and Relaxation", RPI CS78-1, Rensselaer Polytechnic Institute, Troy, New York, 1978.

[9] Davison, L., Stevens, A.L. and Kipp, M.E., "Theory of Spall Damage Accumulation in Ductile Metals", J. Mech. Phys. Solids, 25, 11, 1977.

[10] Budiansky, B., J. Composite Materials, 4, 286, 1970.

[11] Shockey, D.A., Curran, D.R., Austin, M. and Seaman, L., "Development of a Capability for Predicting Cratering and Fragmentation Behavior in Rock", DNA 3730F, Stanford Research Institute, Menlo Park, California, 1975.

APPENDIX A

CODE IMPLEMENTATION OF STEP PULSE PROBLEM

Tension Options

The step pulse problem has been run using the wave code WONDY with the usual solid equation of state routine STAT1 simplified to model a linear elastic material and the three tensile failure options outlined in the text: instantaneous fracture implemented in pure continuum fashion and with local separation of the mesh, and plastic tensile failure. There are three tension model options available in WONDY. The first (FCRIT = 1) suppresses fracture and allows a material to stretch at some energy dependent maximum tensile stress. This option is used directly to model plastic failure with the maximum tensile stress, a constant, equal to the spall strength of the material σ_o. Option 1 can also be used, in modified form, to model instantaneous fracture in a continuum manner. In this case, all stress quantities in a cell are reset to zero when the stress exceeds the spall strength. The second WONDY fracture option (FCRIT = 2) allows two zones to separate whenever the interpolated stress at their common boundary is more tensile than σ_o. This is the non-continuum approach to instantaneous fracture. The third WONDY fracture option (FCRIT = 3) is not tested in the present study. In this option, the value of a cumulative damage integral

$$K = \int_0^t (\sigma - \sigma_o) \ dt,$$

not the stress itself, is compared to a maximum permitted value K_{max}. While the criterion for fracture, $K \geq K_{max}$, is time dependent, the implementation of fracture in terms of cell boundary separation continues to be instantaneous. Stress is not relaxed gradually but rather instantaneously reset to zero when fracture is triggered. Hence option 3 can be expected to share the stability-uniqueness problems of the fully time-independent fracture models being examined.

Non-dimensionalization and Initialization

Since there are no dimensional constants in WONDY, running in non-dimensional form is suggested for parametric studies. A characteristic length L_o along the bar of unit value is chosen as the reference independent variable. The undisturbed density ρ_o and wave speed c_o of the material are the two reference dependent variables selected. All other dependent variables and time are converted to their appropriate non-dimensional forms.

$$\sigma \rightarrow \sigma/\rho_o c_o^2$$

$$\varepsilon \rightarrow \varepsilon/c_o^2$$

$$t \rightarrow tc_o/L_o$$

where ε is the energy per unit mass and for concreteness, ρ_o has been taken as 2.7 gm/cm^3, c_o as 5.0 cm/sec, and σ_o as 2GPa.

The mesh is set up with 100 uniform cells of width 0.02. The step pulse (of width 0.40, compressive stress amplitude s, and density 1-s) is initially at a distance 0.6 from the free end of the bar and traveling toward it, as illustrated in Fig. A1 below.

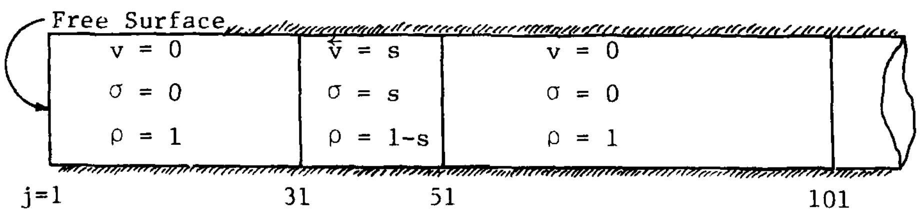

Figure A1. Initialization of Step Pulse Problem

APPENDIX B

DFRACT PRESSURE VOLUME RELATIONS

The equation-of-state routine DFRACT is based on a damage dependent set of pressure-volume relations. Damage in this model is assumed to take the form of spherical voids developing under the influence of tensile pressure (average stress). As detailed in Ref. [4],

$$V = V_s + V_v$$

$$PV = P_s V_s$$

$$P_s = K_o\left(\frac{V_o}{V_s} - 1\right) + \frac{\Gamma E}{V_s}$$

$$dE = -PdV$$

where V is specific gross volume, V_o initial specific gross volume, V_s specific solid volume and V_v specific void volume. The pressure associated with the gross material is P, that with the solid material is P_s. The quantities K_o, Γ and E have their usual meanings i.e., ambient bulk modulus, Grüneisen parameter and internal energy.

The time rate of change of specific void volume is assumed to be caused by void nucleation and void growth

$$\dot{V}_v = \dot{V}_n + \dot{V}_G$$

where, for spherical voids,

$$\dot{V}_n = \begin{cases} 8\pi T_3^3\ T_4 \exp \dfrac{P-T_5}{T_6} & P \geq T_5 \\ 0 & P < T_5 \end{cases}$$

$$\dot{V}_G \approx \begin{cases} T_1(P - T_2)V_v & P \geq T_2 \\ 0 & P < T_2 \end{cases}$$

(P has been assumed positive in tension.)

The relationships between the SRI material parameters, T_1 to T_6, and the constants used in the Weidlinger visco-damage model are listed in Appendix C. Note that the Grüneisen parameter can be set to zero in a given trial to improve the correspondence between the SRI and Weidlinger models.

APPENDIX C

VISCO-DAMAGE MATERIAL PARAMETERS FOR ARMCO IRON AND ALUMINUM

Symbol	Relation to SRI Parameter	Units	Armco Iron	Aluminum
c_n	T_4	No/cm^3/sec	$4.6\text{x}10^{12}$	$3\text{x}10^{9}$
$\mathcal{V}_o$	$\begin{cases} 8\pi T_3^3 \text{(spherical voids)} \\ 32\left(\frac{1-\nu^2}{E}\right) T_5 T_3^3 \text{(planar cracks)} \end{cases}$ E = Young's modulus ν = Poisson's ratio	cm^3	$5\text{x}10^{-13*)}$	$2.3\text{x}10^{-11}$
σ_n	T_5	dyn/cm^2	$3\text{x}10^{9}$	$3\text{x}10^{9}$
σ_1	T_6	dyn/cm^2	$4.6\text{x}10^{9}$	$4\text{x}10^{8}$
c_G	$T_1/3$	cm^2/dyn/sec	$2\text{x}10^{-4}$	$3.3\text{x}10^{-3}$
σ_G	T_2	dyn/cm^2	$2.0\text{x}10^{8}$	$4\text{x}10^{9}$

*) SRI data, Ref. [4], has been used directly for the visco-damage material parameters except in the case of $\mathcal{V}_o$ (Armco). This parameter has been modified in an attempt to compensate for the fact that the nucleation size parameter T_3 has been determined for planar cracks, but is being applied to spherical voids in the Weidlinger model.

DISTRIBUTION LIST

DEPARTMENT OF DEFENSE

Assistant to the Secretary of Defense
Atomic Energy
ATTN: Executive Assistant

Defense Advanced Rsch Proj Agency
ATTN: TIO
ATTN: G. Bulin

Defense Intelligence Agency
ATTN: DB-4N
ATTN: DB-4C, E. O'Farrell

Defense Nuclear Agency
2 cy ATTN: SPSS
4 cy ATTN: TITL

Defense Technical Information Center
12 cy ATTN: DD

Field Command
Defense Nuclear Agency
ATTN: FCPR
ATTN: FCTMOF

Field Command
Defense Nuclear Agency
Livermore Division
ATTN: FCPRL

Interservice Nuclear Weapons School
ATTN: TTV

Joint Strat Tgt Planning Staff
ATTN: NRI-STINFO Library
ATTN: JLA

NATO School (SHAPE)
ATTN: U.S. Documents Officer

Undersecretary of Def for Rsch & Engrg
ATTN: Strategic & Space Systems (OS)

DEPARTMENT OF THE ARMY

BMD Advanced Technology Center
Department of the Army
ATTN: 1CRDABH-X
ATTN: ATC-T

Chief of Engineers
Department of the Army
ATTN: DAEN-MCE-D
ATTN: DAEN-RDM

Harry Diamond Laboratories
Department of the Army
ATTN: DELHD-N-P
ATTN: DELHD-I-TL

U.S. Army Ballistic Research Labs
ATTN: DRDAR-BLV
ATTN: DRDAR-TSB-S
ATTN: DRDAR-BLE, J. Keefer

DEPARTMENT OF THE ARMY (Continued)

U.S. Army Concepts Analysis Agency
ATTN: CSSA-ADL

U.S. Army Engineer Center
ATTN: DT-LRC

U.S. Army Engineer Div, Huntsville
ATTN: HNDED-SR

U.S. Army Engineer Div, Ohio River
ATTN: ORDAS-L

U.S. Army Engr Waterways Exper Station
ATTN: J. Strange
ATTN: WESSA, W. Flathau
ATTN: J. Zelasko
ATTN: WESSE, L. Ingram
ATTN: Library
ATTN: J. Drake
2 cy ATTN: WESSD, J. Jackson

U.S. Army Material & Mechanics Rsch Ctr
ATTN: Technical Library

U.S. Army Materiel Dev & Readiness Cmd
ATTN: DRXAM-TL

U.S. Army Missile Command
ATTN: RSIC

U.S. Army Nuclear & Chemical Agency
ATTN: Library

DEPARTMENT OF THE NAVY

Naval Construction Battalion Center
Civil Engineering Laboratory
ATTN: Code L08A
ATTN: Code L51, R. O'Dello
ATTN: Code L51, S. Takahashi

Naval Electronic Systems Command
ATTN: PME 117-21

Naval Facilities Engineering Command
ATTN: Code 03T
ATTN: Code 04B
ATTN: Code 09M22C

Naval Material Command
ATTN: MAT 08T-22

Naval Postgraduate School
ATTN: Code 0142 Library
ATTN: G. Lindsay

Naval Research Laboratory
ATTN: Code 2627

Naval Surface Weapons Center
ATTN: Code F-31

DEPARTMENT OF THE NAVY (Continued)

Naval Surface Weapons Center
ATTN: Tech Library & Info Services Br

Naval War College
ATTN: Code E-11

Naval Weapons Evaluation Facility
ATTN: Code 10

Officer in Charge
Newport Laboratory
Naval Underwater Systems Center
ATTN: Code EM, J. Kalinowski

Office of Naval Research
ATTN: Code 715
ATTN: Code 474, N. Perrone

Office of the Chief of Naval Operations
ATTN: OP 981
ATTN: OP 03EG

Strategic Systems Project Office
Department of the Navy
ATTN: NSP-43

DEPARTMENT OF THE AIR FORCE

Air Force Geophysics Laboratory
ATTN: LWW, K. Thompson

Air Force Institute of Technology
ATTN: Library

Air Force Office of Scientific Research
ATTN: J. Allen
ATTN: W. Best

Headquarters
Air Force Systems Command
ATTN: DLW

Air Force Weapons Laboratory
Air Force Systems Command
ATTN: NTE, M. Plamondon
ATTN: NTES, R. Jolley
ATTN: NTES, J. Thomas
ATTN: NTES-C, R. Henny
ATTN: SUL

Asst Chief of Staff
Intelligence
Department of the Air Force
ATTN: INT

Ballistic Missile Office
Air Force Systems Command
ATTN: MNNXH, D. Gage
ATTN: MNN
ATTN: MNNXH, M. Delvecchio

Deputy Chief of Staff
Logistics & Engineering
Department of the Air Force
ATTN: LEEE

DEPARTMENT OF THE AIR FORCE (Continued)

Research, Development & Acq
Department of the Air Force
ATTN: AFRDQSM

Foreign Technology Division
Air Force Systems Command
ATTN: NIIS Library

Rome Air Development Center
Air Force Systems Command
ATTN: TSLD

Strategic Air Command/XPFS
Department of the Air Force
ATTN: NRI-STINFO Library

VELA Seismology Center
ATTN: G. Ullrich

DEPARTMENT OF ENERGY

Department of Energy
Albuquerque Operations Office
ATTN: CTID

Department of Energy
Nevada Operations Office
ATTN: Mail & Records for Tech Library

DEPARTMENT OF ENERGY CONTRACTORS

Lawrence Livermore National Laboratory
ATTN: Tech Info Dept Library

Los Alamos National Scientific Lab
ATTN: MS 364
ATTN: R. Bridwell
ATTN: MS 670, J. Hopkins

Oak Ridge National Laboratory
ATTN: Civil Def Res Proj
ATTN: Central Research Library

Sandia National Labs
ATTN: 3141
ATTN: A. Chabai
ATTN: L. Hill

Sandia National Labs
Livermore Lab
ATTN: Library & Security Class Div

OTHER GOVERNMENT AGENCIES

Central Intelligence Agency
ATTN: OSWR/NED

Department of the Interior
Bureau of Mines
ATTN: Tech Library

Federal Emergency Management Agency
ATTN: Hazard Eval & Vul Red Div

DEPARTMENT OF DEFENSE CONTRACTORS

Aerospace Corp
ATTN: Technical Info Services

Agbabian Associates
ATTN: M. Agbabian

Applied Theory, Inc
2 cy ATTN J. Trulio

AVCO Research & Systems Group
ATTN: Library A830

BDM Corp
ATTN: T. Neighbors
ATTN: Corporate Library

Boeing Company
ATTN: Aerospace Library

California Institute of Tech
ATTN: T. Ahrens

California Research & Technology, Inc
ATTN: M. Rosenblatt
ATTN: S. Schuster
ATTN: Library
ATTN: K. Kreyenhagen

California Research & Tech, Inc
ATTN: D. Orphal

Calspan Corp
ATTN: Library

University of Denver
Colorado Seminary
ATTN: J. Wisotski

EG&G Washington Analytical Srv Center, Inc
ATTN: Library

Eric H. Wang
Civil Engineering Rsch Fac
ATTN: N. Baum

Gard, Inc
ATTN: G. Neidhardt

General Electric Company—TEMPO
ATTN: DASIAC

Higgins, Auld & Associates
ATTN: N. Higgins
ATTN: H. Auld
ATTN: J. Bratton

Higgins, Auld & Associates, Inc
ATTN: S. Blouin

IIT Research Institute
ATTN: Documents Library
ATTN: M. Johnson
ATTN: R. Welch

DEPARTMENT OF DEFENSE CONTRACTORS (Continued)

Institute for Defense Analyses
ATTN: Classified Library

J. H. Wiggins Company, Inc
ATTN: J. Collins

Kaman AviDyne
ATTN: N. Hobbs
ATTN: Library

Kaman Sciences Corp
ATTN: Library

Lockheed Missiles & Space Co, Inc
ATTN: T. Geers
ATTN: Tech Info Center

Lovelace Biomedical & Env Rsch Inst, Inc
ATTN: R. Jones

McDonald Douglas Corp
ATTN: R. Halprin

Merritt CASES, Inc
ATTN: J. Merritt
ATTN: Library

Nathan M. Newmark Consult Eng Svcs
ATTN: N. Newmark

Physics International Company
ATTN: Technical Library
ATTN: E. Moore
ATTN: L. Behrmann
ATTN: F. Sauer
ATTN: J. Thomsen

R & D Associates
ATTN: J. Lewis
ATTN: J. Carpenter
ATTN: W. Wright, Jr
ATTN: R. Port
ATTN: C. MacDonald
ATTN: Tech Info Center
ATTN: P. Haas

Science Applications, Inc
ATTN: Technical Library

Science Applications, Inc
ATTN: D. Maxwell
ATTN: D. Bernstein

Science Applications, Inc
ATTN: W. Layson

Southwest Research Institute
ATTN: W. Baker
ATTN: A. Wenzel

Systems, Science & Software, Inc
ATTN: J. Murphy

DEPARTMENT OF DEFENSE CONTRACTORS (Continued)

SRI International
ATTN: Y. Gupta
ATTN: G. Abrahamson
ATTN: B. Gasten
ATTN: D. Keough

Systems, Science & Software, Inc
ATTN: T. Riney
ATTN: D. Grine
ATTN: Library
ATTN: T. Cherry

Terra Tek, Inc
ATTN: S. Green
ATTN: A. Abou-Sayed
ATTN: Library

Tetra Tech, Inc
ATTN: L. Hwang
ATTN: Library

DEPARTMENT OF DEFENSE CONTRACTORS (Continued)

TRW Defense & Space Sys Group
ATTN: P. Bhutta
ATTN: Tech Information Center
2 cy ATTN: N. Lipner

TRW Defense & Space Sys Group
ATTN: P. Dai
ATTN: E. Wong

Universal Analytics, Inc
ATTN: E. Field

Weidlinger Assoc, Consulting Engineers
ATTN: M. Baron

Weidlinger Assoc, Consulting Engineers
ATTN: J. Isenberg

DAT

FILM

3